HAL
open science

Treatment of HCC with claudin-1-specific antibodies suppresses carcinogenic signaling and reprograms the tumor microenvironment

Natascha Roehlen, Marion Muller, Zeina Nehme, Emilie Crouchet, Frank Jühling, Fabio del Zompo, Sara Cherradi, François Ht Duong, Nuno Almeida, Antonio Saviano, et al.

To cite this version:

Natascha Roehlen, Marion Muller, Zeina Nehme, Emilie Crouchet, Frank Jühling, et al.. Treatment of HCC with claudin-1-specific antibodies suppresses carcinogenic signaling and reprograms the tumor microenvironment. Journal of Hepatology, 2023, 78 (2), pp.343-355. 10.1016/j.jhep.2022.10.011 . hal-04017104

HAL Id: hal-04017104

https://hal.science/hal-04017104v1

Submitted on 6 Mar 2023

HAL is a multi-disciplinary open access archive for the deposit and dissemination of scientific research documents, whether they are published or not. The documents may come from teaching and research institutions in France or abroad, or from public or private research centers.

L'archive ouverte pluridisciplinaire **HAL**, est destinée au dépôt et à la diffusion de documents scientifiques de niveau recherche, publiés ou non, émanant des établissements d'enseignement et de recherche français ou étrangers, des laboratoires publics ou privés.

Research Article
Hepatic and Biliary Cancer

JOURNAL
OF HEPATOLOGY

Treatment of HCC with claudin-1-specific antibodies suppresses carcinogenic signaling and reprograms the tumor microenvironment

Authors

Natascha Roehlen, Marion Muller, Zeina Nehme, …, Catherine Schuster, Laurent Mailly, Thomas F. Baumert

Correspondence

thomas.baumert@unistra.fr (T.F. Baumert).

Graphical abstract

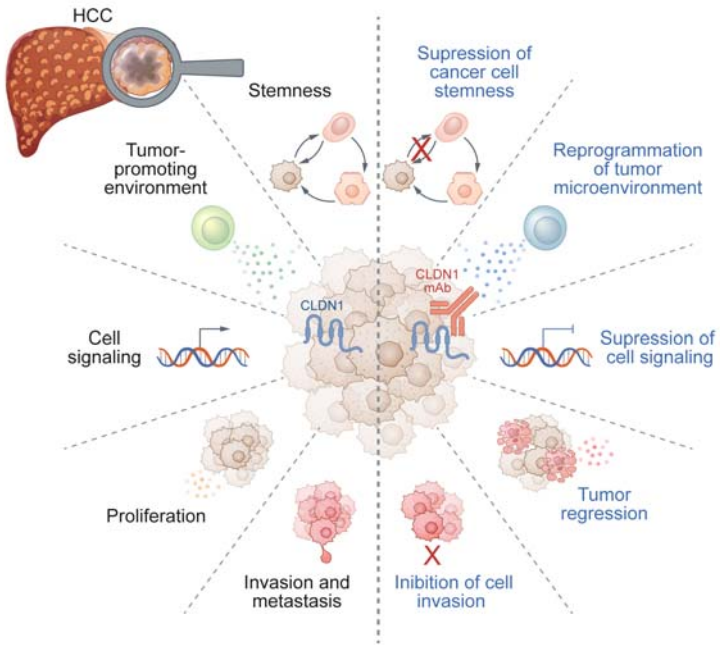

Highlights

- CLDN1 is upregulated in HCC and is associated with stemness and an immune-low tumor microenvironment.
- A mAb targeting non-junctional CLDN1 suppresses tumor growth and invasion in patient-derived cell-based and *in vivo* models.
- This mAb perturbs interactions of CLDN1 with signaling proteins, including Notch ligand JAG1.
- We provide robust pre-clinical proof-of-concept for a first-in-class CLDN1 mAb for the treatment of advanced HCC.

Impact and implications

Hepatocellular carcinoma (HCC) is associated with high mortality and unsatisfactory treatment options. Herein, we identified the cell surface protein Claudin-1 as a treatment target for advanced HCC. Monoclonal antibodies targeting Claudin-1 inhibit tumor growth in patient-derived *ex vivo* and *in vivo* models by modulating signaling, cell stemness and the tumor immune microenvironment. Given the differentiated mechanism of action, the identification of Claudin-1 as a novel therapeutic target for HCC provides an opportunity to break the plateau of limited treatment response. The results of this preclinical study pave the way for the clinical development of Claudin-1-specific antibodies for the treatment of advanced HCC. It is therefore of key impact for physicians, scientists and drug developers in the field of liver cancer and gastrointestinal oncology.

https://doi.org/10.1016/j.jhep.2022.10.011
© 2022 The Authors. Published by Elsevier B.V. on behalf of European Association for the Study of the Liver. This is an open access article under the CC BY-NC-ND license (http://creativecommons.org/licenses/by-nc-nd/4.0/). J. Hepatol. 2023, 78, 343–355

Research Article
Hepatic and Biliary Cancer

JOURNAL OF HEPATOLOGY

Treatment of HCC with claudin-1-specific antibodies suppresses carcinogenic signaling and reprograms the tumor microenvironment

Natascha Roehlen[1,2], Marion Muller[1,2,3], Zeina Nehme[1,2], Emilie Crouchet[1,2], Frank Jühling[1,2], Fabio Del Zompo[1,2], Sara Cherradi[1,2], Francois H.T. Duong[1,2], Nuno Almeida[1,2], Antonio Saviano[4], Mirian Fernández-Vaquero[5], Tobias Riedl[5], Houssein El Saghire[2,6], Sarah C. Durand[1,2], Clara Ponsolles[1,2], Marine A. Oudot[1,2], Romain Martin[1,2], Nicolas Brignon[1,2], Emanuele Felli[4], Patrick Pessaux[4], Antonin Lallement[1,2,7], Irwin Davidson[7], Simonetta Bandiera[1,2], Christine Thumann[1,2], Patrice Marchand[1,3], Solange Moll[8], Brandon Nicolay[9], Nabeel Bardeesy[9], Yujin Hoshida[10], Mathias Heikenwälder[5], Roberto Iacone[6], Alberto Toso[6], Markus Meyer[6], Greg Elson[6], Tamas Schweighoffer[6], Geoffrey Teixeira[6], Mirjam B. Zeisel[1,2,11], Patrice Laquerriere[1,3], Joachim Lupberger[1,2], Catherine Schuster[1,2], Laurent Mailly[1,2], Thomas F. Baumert[1,2,4,12,*]

Journal of Hepatology **2023**. vol. 78 | 343–355

Background & Aims: Despite recent approvals, the response to treatment and prognosis of patients with advanced hepatocellular carcinoma (HCC) remain poor. Claudin-1 (CLDN1) is a membrane protein that is expressed at tight junctions, but it can also be exposed non-junctionally, such as on the basolateral membrane of the human hepatocyte. While CLDN1 within tight junctions is well characterized, the role of non-junctional CLDN1 and its role as a therapeutic target in HCC remains unexplored.
Methods: Using humanized monoclonal antibodies (mAbs) specifically targeting the extracellular loop of human non-junctional CLDN1 and a large series of patient-derived cell-based and animal model systems we aimed to investigate the role of CLDN1 as a therapeutic target for HCC.
Results: Targeting non-junctional CLDN1 markedly suppressed tumor growth and invasion in cell line-based models of HCC and patient-derived 3D *ex vivo* models. Moreover, the robust effect on tumor growth was confirmed *in vivo* in a large series of cell line-derived xenograft and patient-derived xenograft mouse models. Mechanistic studies, including single-cell RNA sequencing of multicellular patient HCC tumorspheres, suggested that CLDN1 regulates tumor stemness, metabolism, oncogenic signaling and perturbs the tumor immune microenvironment.
Conclusions: Our results provide the rationale for targeting CLDN1 in HCC and pave the way for the clinical development of CLDN1-specific mAbs for the treatment of advanced HCC.

© 2022 The Authors. Published by Elsevier B.V. on behalf of European Association for the Study of the Liver. This is an open access article under the CC BY-NC-ND license (http://creativecommons.org/licenses/by-nc-nd/4.0/).

Introduction

Hepatocellular carcinoma (HCC) is a major public health burden and the fourth leading, and rapidly increasing, cause of cancer-related death worldwide.[1] HCC typically develops on the background of advanced liver fibrosis caused by viral or metabolic injury. Irrespective of etiology, hyperactivation of oncogenic signaling such as the Ras/Raf/MAPK, PI3K/AKT/–mTOR, Notch and Wnt/β-catenin pathways are common events involved in HCC initiation and progression. Moreover, the tumor microenvironment (TME) plays a key role in determining HCC outcomes.[1]

Current treatment options for advanced HCC are still unsatisfactory due to limited response rates.[1,2] Therapeutic resistance to current systemic therapies has been associated with tumor cell plasticity, such as epithelial-mesenchymal transition (EMT) and stemness, as well as an immune-exhausted or immune-excluded TME.[1,3,4] Persistence of pro-tumorigenic signals within the fibrotic niche on the other hand accounts for the high risk of tumor recurrence following curative treatment approaches.[1] Collectively, there is an urgent unmet medical need for novel HCC therapeutics that address the drawbacks of drug resistance and tumor recurrence.

Claudin-1 (CLDN1) is a transmembrane protein expressed in tight junctions (TJs) as well as outside of the TJs (non-junctional CLDN1 [NJ-CLDN1]), *e.g.* at the basolateral membrane of the human hepatocyte. Interestingly, NJ-CLDN1 serves as a cell entry factor and signal transducer of HCV,[5] a major cause

Keywords: Liver cancer; tight junction; CLDN1; HCC; plasticity; resistance; stemness; tumor immune microenvironment.
Received 21 February 2022; received in revised form 7 October 2022; accepted 10 October 2022; available online 27 October 2022
* Corresponding author. Address: Inserm U1110, Institut de Recherche sur les Maladies Virales et Hépatiques, Université de Strasbourg, 3 rue Koeberlé, 67000 Strasbourg, France.
E-mail address: thomas.baumert@unistra.fr (T.F. Baumert).
https://doi.org/10.1016/j.jhep.2022.10.011

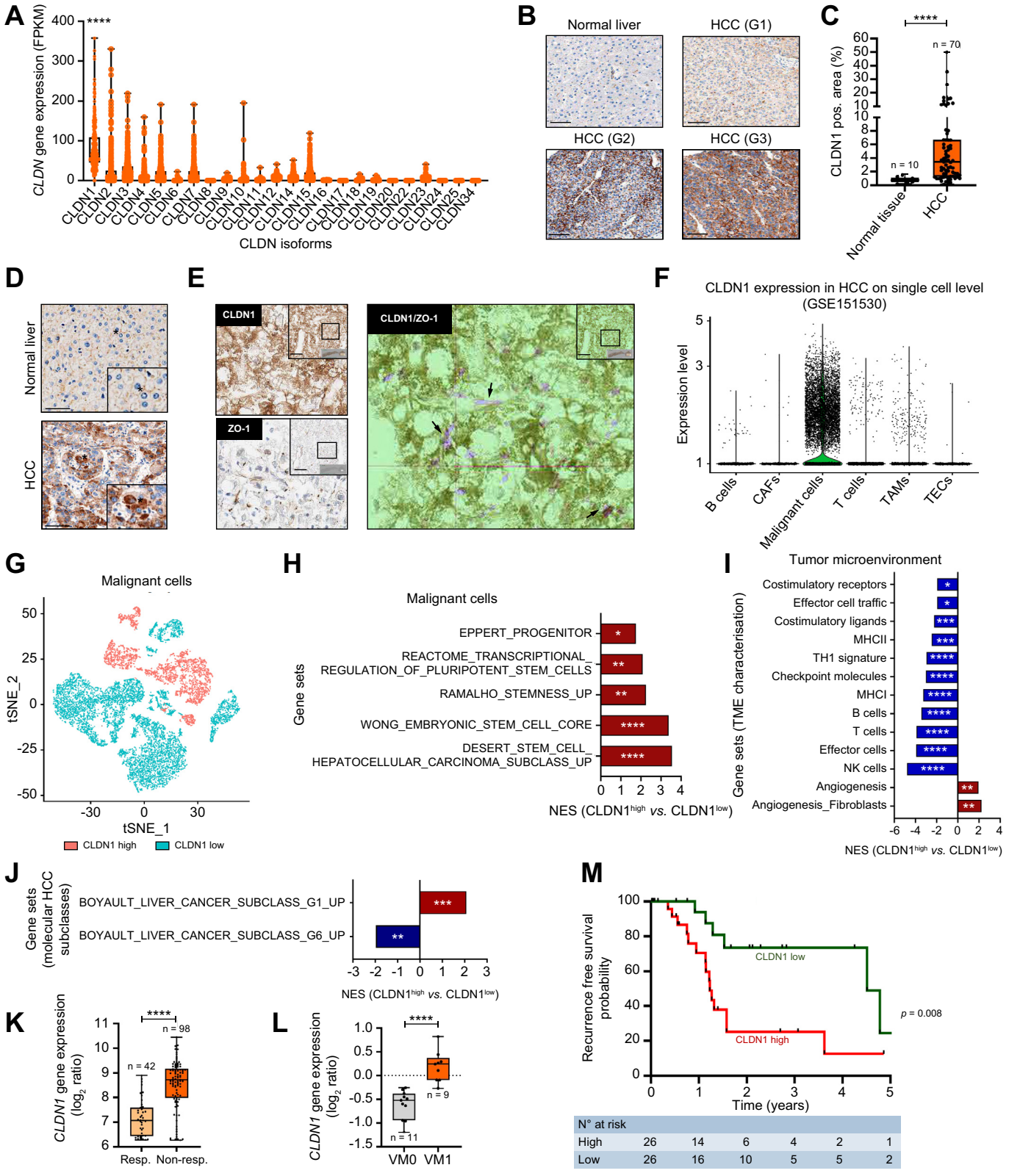

Fig. 1. CLDN1 expression is upregulated in HCC and correlates with stemness and an immune-low tumor microenvironment. (A) Expression of claudin family members in the TCGA cohort (n = 365 patients, p <0.0001, one-way ANOVA). (B–C) Immunostaining of CLDN1 in healthy (n = 10) and HCC tissues (n = 70) of different tumor grades. (B) Representative images (C) quantification (p <0.0001, Mann-Whitney U test). Scale bars 100 μm. (D) Representative high magnification images indicate aberrant NJ localization of CLDN1 in HCC compared to primarily junctional localization in healthy tissue. Scale bars 50 μm. (E) Left panels: Immunostainings of CLDN1 and ZO-1 in consecutive sections of HCC liver tissues. Right panel: Co-staining of CLDN1 (brown) and ZO1 (violet). Scale bars 150 μm (F) CLDN1 expression on single cell level (GSE151530, n = 14 different HCC tissues) shown as violin plots. (G) t-SNE graphs of tumor cells included in GSE151530/CLDN1^{low} or CLDN1^{high}. (H)

of HCC worldwide. Using humanized monoclonal antibodies (mAb) that selectively target NJ-CLDN1, we aimed to study the role of NJ-CLDN1 in tumor progression, plasticity, metabolism and signaling.

Materials and methods

Human samples and patient cohorts

Human liver tissue samples for *ex vivo* perturbation studies were derived from patients with liver resections at the Pôle Hépato-digestif, Strasbourg University Hospitals (2014-2021). All patients provided written informed consent within the ethical principles of the declaration of Helsinki, approved by the local and national ethics committee (*comités de protection des personnes,* protocol RIPH2, LivMod-IDRCB 2019-A00738-49, ClinicalTrial NCT04690972). Sampling of human liver tissue for immunostaining was conducted by *Charles River Laboratories* and *US Biomax Inc*. with informed consent of all donors and under HIPPA approved protocols. Demographic data and clinical characteristics of patients enrolled are summarized in Table S1-3.

Mouse models

Hepa 1.6 mouse model: 8-10-week-old female C57BL/6 J mice were used for *in vivo* CLDN1 gain-of-function studies, using engineered Hepa 1.6 cell line. Experiments were performed at WuXi Apptec, China, in accordance with the local regulations.

Cell line-derived xenograft (CDX) mouse models: 7-10-week-old female and male non-obese diabetic *Rag1*$^{-/-}$*Il2rgc*$^{-/-}$ (NRG) mice were used for all CDX mouse models. Experiments were performed at the animal facility of Inserm U1110 (approval number E67-482-7) according to local laws, ethics committee approval and authorization by the French Ministry of Research and Higher Education (APAFIS #10892-2017080511379629v3, #22327-2019100815074277v3 and #27709-2020101514256404v4). PET scan assessments were performed on CDX mouse models at the animal facility of Institut Pluridisciplinaire Hubert Curien according to local laws and ethics committee approval (APAFiS#26596-2020071609156326v3).

Patient-derived xenograft (PDX) mouse model: 7-week-old female BALB/c nude mice were used with experiments performed at Crown Bioscience, Inc. The protocols were reviewed and approved by the Institutional Animal Care and Use Committee of CrownBio prior to execution. Mice were randomly assigned to the study groups. For details on methodology, please see the supplementary information.

Results

CLDN1 is overexpressed in an HCC subtype characterized by a progenitor phenotype and an "immune-low" type of TME

To investigate the role of CLDN1 in HCC, we first analyzed CLDN1 mRNA and protein levels in individuals with HCC. Computational analysis of data retrieved from Genomic Data Commons Data Portal and the human protein atlas[6] revealed that CLDN1 is the most highly expressed Claudin family member in HCC at both the mRNA (p <0.0001, Fig. 1A) and protein levels (Fig. S1A). Indeed, ∼75% of liver tumors show medium or high CLDN1 expression (Fig. S1A). Moreover, CLDN1 is significantly upregulated in pre-malignant dysplastic nodules of cirrhotic liver (GSE102383, p = 0.03, Fig. S1B), as well as HCC tissue compared to matched non-tumorous adjacent liver (GSE113996, p = 0.02, Fig. S1C). Immunostaining of CLDN1 in healthy and HCC tissue confirmed CLDN1 overexpression, particularly in high grade tumors (p <0.0001, Fig. 1B-C; p = 0.06, Fig. S1D, Table S3). Interestingly, CLDN1 showed aberrant non-junctional localization in HCC in contrast to primarily junctional localization in healthy liver tissue (Fig. 1D). The predominantly non-junctional localization of CLDN1 in HCC tissues was further confirmed by double immunohistochemistry showing absent co-localization of CLDN1 with TJ protein ZO-1 (Fig. 1E).

HCC is characterized by a strong intra- and inter-tumoral heterogeneity and various molecular phenotypes.[1] Characterization of CLDN1 expression in a large HCC single-cell RNA sequencing (scRNAseq) dataset revealed that tumor cells are the key cell population with robust CLDN1 expression (Fig. 1F, Fig. S2A-B). Gene set enrichment analysis (GSEA) revealed that highly CLDN1-expressing tumor cells (Fig. 1G, Fig. S2C-D) exhibited a progenitor or stem cell-like phenotype (false discovery rate [FDR] <0.05, Fig. 1H). Similar results were obtained in various independent large HCC patient cohorts with available bulk transcriptomic data (GSE5975, p <0.0001, Fig. S2E, GSE112791, FDR <0.001, Fig. S2F).

ScRNAseq data from HCC tumors revealed a paucity of immune cells and suppression of immune signatures in tumors with low CLDN1 expression in tumor cells (FDR <0.05, Fig. 1I, Fig. S3A-B), suggesting a functional impact of CLDN1 expression on the tumor immune microenvironment (TIME). Signatures of angiogenesis and desmoplastic reaction on the other hand were significantly induced (FDR <0.01, Fig. 1I). Similar results were obtained in an independent large patient cohort on the bulk transcriptomic level (GSE112791, FDR =

Enrichment of gene sets related to stemness and progenitor cells in CLDN1^{high} tumor cells (GSE151530, FDR <0.05, Kolmogorov-Smirnov test). (I) Enrichment of gene sets related to an immune-enriched or immune-active tumor immune microenvironment in tumors with low CLDN1 expression. Bars indicate NES of significant enrichments (GSE151530, FDR <0.05, Kolmogorov-Smirnov test). (J) Enrichment of genes specific for Boyault Liver Cancer Subclass G1 in tumors with high CLDN1 expression (GSE20140, n = 164 FDR <0.001, Kolmogorov-Smirnov-test). (K) *CLDN1* expression in HCC tissue predicted to confer response (n = 42) or resistance (n = 98) to sorafenib treatment (GSE109211, p <0.0001, Student's t test). (L) *CLDN1* mRNA expression in the non-cancerous tumor-microenvironment of individuals with HCC with (VM1, n = 9) or without (VM0, n = 11) venous metastasis (GSE5093, p <0.0001, Mann-Whitney U test). (M) Recurrence-free survival in individuals with high (50% above median, n = 26) *vs.* low (50% below median, n = 26) *CLDN1* expression in tumor adjacent liver tissue (GSE76427, p = 0.008, log rank test). Boxplots represent median (—), 1st and 3rd quartile (bottom and top of the box) and single data points (•). Vertical bars show NES of significantly (FDR <0.05, Kolmogorov-Smirnov test) altered gene sets. *p <0.05, **p <0.01, ***p <0.001, ****p <0.0001. FDR, false discovery rate; FPKM, fragments per kilobase million; HCC, hepatocellular carcinoma; HpSC-HCC, progenitor-like stem cell signature; MH-HCC, hepatocyte mature HCC; NES, normalized enrichment score; NJ, non-junctional; VM0, HCC adjacent tissue without venous metastasis; VM1, HCC adjacent tissue with venous metastasis; t-SNE, t-distributed stochastic neighbor embedding.

0.04, Fig. S3C). As expected, given the correlation with a progenitor phenotype and an immune-low or -excluded TME, HCCs with high CLDN1 expression showed enrichment for genes specific for the Boyault G1 subclass of HCC[7] (FDR <0.001, Fig. 1J). While we did not detect an association of CLDN1 expression in HCC tumors with survival (Fig. S3D), the association with transcriptomic signatures of sorafenib resistance[8] supports a prognostic function of CLDN1 (GSE109211, p <0.0001, Fig. 1K). Furthermore, high *CLDN1* expression in HCC adjacent liver tissue was associated with metastatic behavior of the corresponding tumor and with worse post-resection recurrence-free survival (GSE5093, p <0.0001, Fig. 1L, GSE76427, p = 0.008, Fig. 1M). Collectively, these data suggest that CLDN1 is a potential hallmark for tumor cell differentiation and TIME.

Genetic driver mutations, TNF-α/NF-κB and hypoxia upregulate CLDN1 overexpression that accelerates tumor growth *in vivo*

We next screened a large group of different cytokines, growth factors and conditions to identify molecular drivers of CLDN1 overexpression in HCC. We found hypoxia and TNF-α/NF-κB to strongly upregulate CLDN1 expression in the human Huh7 HCC cell line (p = 0.03, Fig. 2A-B). Moreover, assessment of CLDN1 expression dependent on genetic driver mutations in the TCGA liver cancer cohort revealed AXIN1 mutations to be associated with CLDN1 upregulation (p = 0.003, Fig. S4), whereas CTNNB1 mutations were found to be associated with CLDN1 downregulation (p <0.0001, Fig. S4). This is in line with CLDN1 being associated with the G1 Boyault HCC subclassification that is linked to AXIN1 mutations.[7] Finally, CLDN1 gain-of-function in mouse Hepa1.6 HCC cells that do not endogenously express CLDN1 (Fig. 2C) led to accelerated tumor growth when subcutaneously injected into syngeneic C57BL/6 J mice (p = 0.008, Fig. 2D), validating the pro-tumorigenic phenotype of CLDN1 overexpression *in vivo*.

CLDN1 mAb suppresses tumor growth and EMT in patient-derived *ex vivo* models

Given the upregulation of NJ-CLDN1 in HCC (Fig. 1D-E), we studied its role as a therapeutic target for HCC using a fully humanized mAb directed against the first extracellular loop of CLDN1.[5] Flow cytometry revealed robustly enhanced binding of CLDN1 mAb to patient-derived tumor cells compared to matched adjacent liver non-tumoral cells (p = 0.004, Wilcoxon signed-rank test, Fig. S5).

Treatment of human hepatoma cell lines Huh7 and Hep3B with a CLDN1 mAb significantly inhibited tumor sphere formation, growth and invasion (Fig. S6A-C). We next assessed the effect of the CLDN1 mAb on tumor growth in a fully

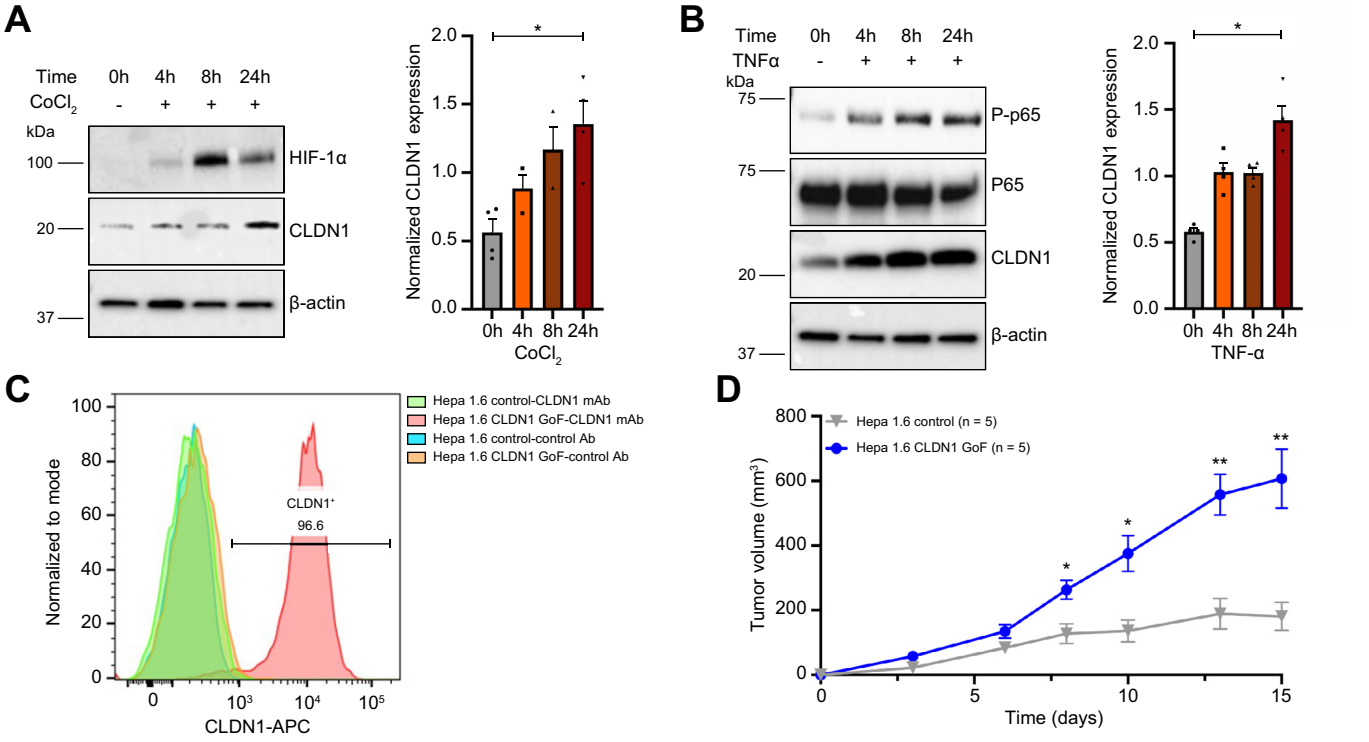

Fig. 2. Regulation of CLDN1 expression by hypoxia and effect of CLDN1 overexpression on tumor growth in a syngeneic mouse model. (A, B) Upregulation of CLDN1 expression by hypoxia and TNFα. (A) Left panel: representative immunoblots of HIF1α, CLDN1 and β-actin in Huh7 cells treated with cobalt chloride for 0, 4, 8 and 24 h. Right panel: Normalized CLDN1 expression (n = 3; p = 0.03, Mann-Whitney U test). (B) TNFα–NF–κB. Left panel: Representative immunoblots of phospho-p65, p65, CLDN1 and β-actin in Huh7 cells treated with TNFα for 0, 4, 8 and 24 h. Right panel: Normalized CLDN1 expression upon stimulation with TNF (n = 3, p = 0.03, Mann-Whitney U test). (C, D) Tumor growth in a CLDN1 syngeneic mouse model engrafted with wild-type and CLDN1-overexpressing Hepa1.6 cells (GoF). (C) Expression of cell surface CLDN1 in wild-type or CLDN GoF Hepa1.6 cells. Shown are representative histograms of fluorescence intensity in Hepa1.6 cells stained with CLDN1 mAb or control. (D) Tumor volume in n = 5 mice per group was monitored over 15 days (*p <0.05, **p <0.01, Mann-Whitney U test). Bars show mean±SEM and single data points. GoF, gain of function; mAb, monoclonal antibody.

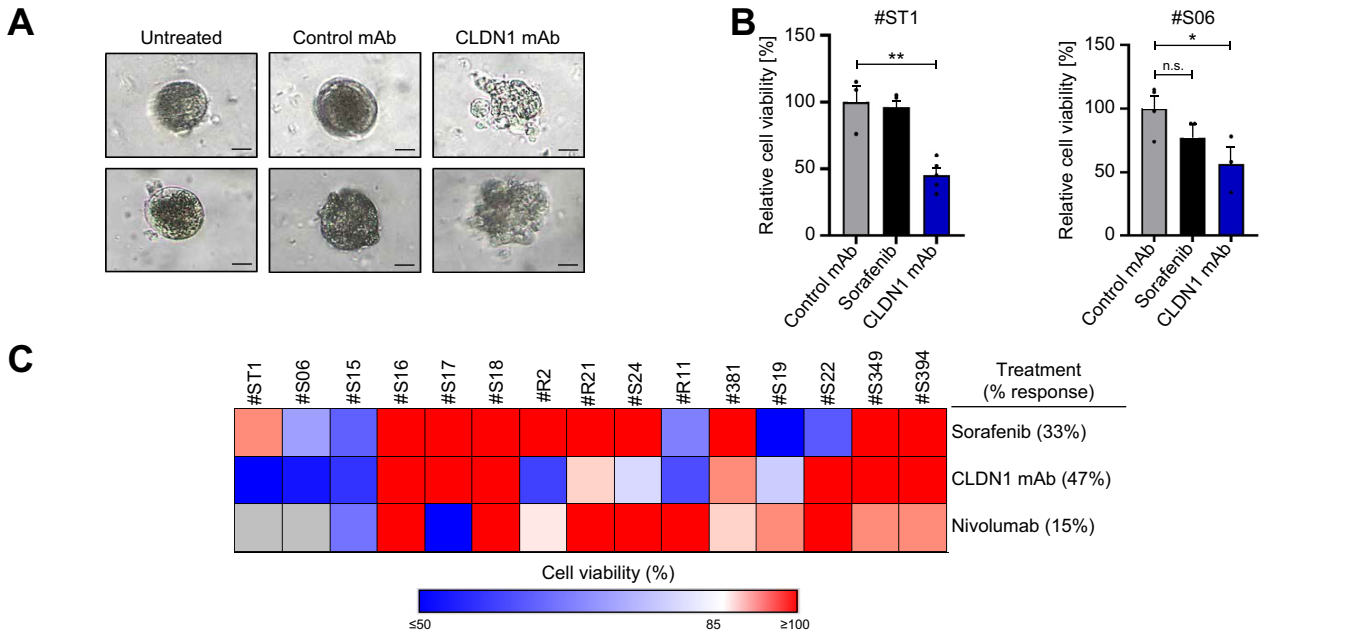

Fig. 3. Treatment with CLDN1 mAb reduces viability in patient-derived *ex vivo* models of HCC. (A) Representative microscopic photos of tumor spheroids generated from HCC liver tissue treated with CLDN1 or control mAb on day 6 post-treatment are shown. Scale bars 200 μm. (B) Relative cell viability after 6 days of treatment with CLDN1 mAb or sorafenib compared to control mAb treated spheroids (n = 3 replicates per condition, $p = 0.003$ and $p = 0.04$, Student's *t* test). (C) Tumor spheroids (n = 15 donors) were treated with CLDN1 mAb, control Ab, sorafenib or nivolumab. Heatmaps illustrate % cell viability compared to control mAb treated cells on day 6 using ATP quantification (n = 15 different donors with at least duplicates per condition). (•). Bars show mean ±SEM. *p <0.05, **p <0.01, ***p <0.001, ****p <0.0001. CAFs, cancer-associated fibroblasts; ECM, extracellular matrix; HCC, hepatocellular carcinoma; mAb, monoclonal antibody.

patient-derived culture system, modeling tumor heterogeneity. Cultured as multicellular micro-tissues, primary HCC tumorspheres maintain original cell-cell contacts and recapitulate non-parenchymal cells of the TME, including T cells, which are relevant for tumor progression and therapeutic resistance.[9] CLDN1 mAb treatment markedly disrupted the architecture of HCC spheroids (Fig. 3A). Moreover, the CLDN1 mAb showed a pronounced effect on sorafenib-resistant HCC spheroid cell viability[1] (donor #ST1 $p = 0.003$ and #S06 $p = 0.04$, Fig. 3B). A subsequent screen in HCC spheroids derived from 15 different patients with HCC (patients' characteristics shown in Table S1), corroborated the effects of the CLDN1 mAb on tumor cell viability, with superior response rates compared to sorafenib and nivolumab (47% *vs.* 33% and 15%, respectively, defined as a mean decrease in cell viability of >15%, Fig. 3C).

Collectively, these data indicate strong suppressive effects of the CLDN1 mAb on HCC growth, including on sorafenib- and nivolumab-resistant tumors.

CLDN1 mAb suppresses tumor growth in both CDX and PDX mouse models

We next assessed the effect of the mAb on tumor growth in Huh7 and Hep3B CDX mouse models (Fig. 4A). The CLDN1-specific mAb significantly reduced tumor growth *in vivo* (Fig. 4B, Fig. S7A). The CLDN1 mAb antagonized tumor cell proliferation as measured by a strong reduction in the percentage of KI67+ cells (Fig. 4C). Assessment of caspase 3 cleavage and TUNEL suggested pro-apoptotic effects ($p = 0.002$, Fig. 4D, Fig. S7B).

We next used PDX mouse models to partially recapitulate tumoral heterogeneity and predict clinical outcomes[10] to evaluate the anti-tumoral efficacy of the CLDN1 mAb. Following established tumor growth, mice from 6 different PDX mouse models (Table S2; Fig. 4E) were randomized into groups receiving weekly i.p. injections of CLDN1 mAb (n = 3 per model) or vehicle control (n = 2 per model). Treatment with CLDN1 mAb suppressed tumor growth by 38.5% on average in 4 out of 6 PDX models within 28 days of treatment, a response rate superior to currently approved treatment in clinical practice[1] (Fig. 4F-G). The observed inhibition was confirmed in a second study with an increased number of mice per group showing highly significant, dose-dependent inhibition of HCC growth (Fig. 4H). Similar to CDX mice, CLDN1 mAb treatment induced apoptosis as shown by Caspase 3 cleavage ($p = 0.01$, Fig. S7C). Body weight in CLDN1 mAb-treated animals remained unaltered compared to the control group throughout the study (Table S4).

RNA-sequencing (RNA-seq) and GSEA performed on pre-treatment PDX HCC tissues revealed that Wnt/β-catenin, Hedgehog and EMT signatures were strongly enriched in responders, irrespective of both tumor grade and histological features (Fig. 4I). Interestingly, treatment resistance was associated with MYC and oxidative stress signatures. Similar results were obtained in tumor samples, whose response to CLDN1 mAb therapy was evaluated in HCC spheroids (Fig. 4I), validating the predictive values of the PDX signatures. Interestingly, tumors that responded to the CLDN1 mAb showed enrichment of transcriptomic signatures predicting a fibrotic and immune-enriched microenvironment (FDR = 0.03 and 0.01, respectively, Fig. 4J). Collectively, these data provide robust preclinical proof-of-concept for the treatment of HCC with CLDN1 mAbs and suggest a functional role of the TIME in treatment response.

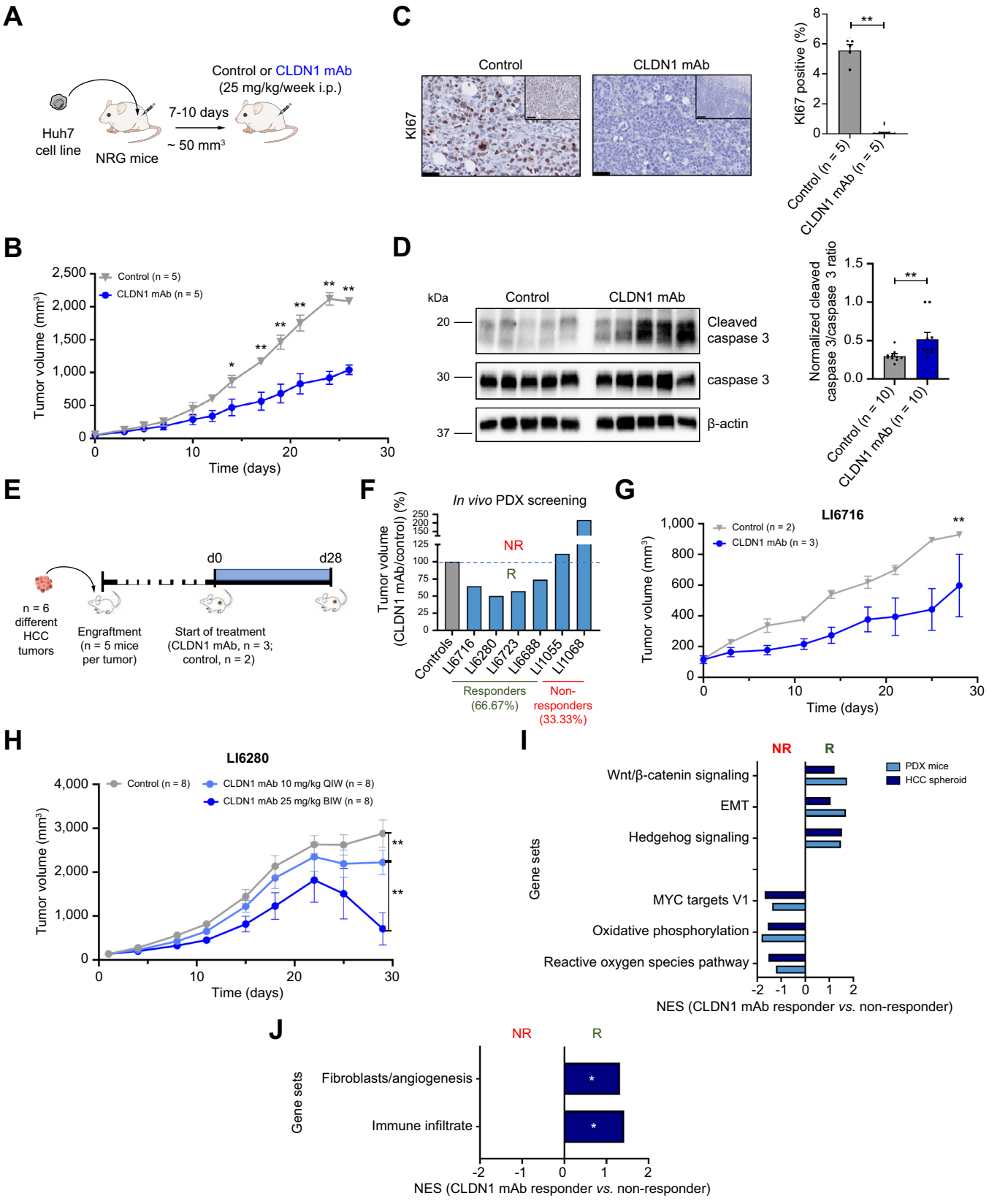

Fig. 4. CLDN1 mAb inhibits tumor growth in CDX and PDX mouse models of HCC. (A) Huh7 CDX mouse model study protocol (two independent studies). (B) Tumor growth (n = 5 mice per group, *p <0.05, **p <0.01, Mann-Whitney test). (C) Immunohistochemistry and quantification of KI67 expression in tumor tissues. Scale bars - 1 mm and 200 μm (**p <0.01, Mann-Whitney U test). (D) Tumor apoptosis. Left panel: representative immunoblots of cleaved caspase 3, caspase 3 and β-Actin. Right panel: quantification of normalized cleaved caspase/caspase 3 ratio in tumor tissues (two different lysates for n = 5 mice; p = 0.002, Mann-Whitney U test). (E) PDX mouse model study protocol (6 independent studies with n = 6 different HCC tumors). (F) The relative mean tumor volume (%) in CLDN1 mAb- (n = 3 mice per

CLDN1 mAb interferes with oncogenic signaling and suppresses cancer cell metabolism *in vivo*

To gain further insights into the molecular mechanisms that underlie the anti-tumor growth effect of CLDN1 mAbs, we next performed RNA-seq and GSEA on the PDX responder #LI6716 (Fig. 4G). CLDN1 has previously been reported to regulate intracellular signaling cascades by forming multi-protein complexes at the membrane.[11] Corroborating the role of exposed NJ-CLDN1 as a signaling hub, mice treated with CLDN1 mAb showed strong suppression of several key oncogenic signaling pathways, with the strongest effects on TNF-α/NF-κB, TGF-β, IL-6/JAK/STAT3, KRAS and Wnt/β-catenin signaling (Fig. 5A). Validating the specificity of these results, suppression of canonical TNF-α and TGF-β signaling via p65 and SMAD2/3 was observed intermodally in CDX mice at the protein level ($p = 0.04$ and 0.03, respectively, Fig. 5B-C, Fig. S8). Interestingly, transcriptomic analysis further revealed a strong suppression of hypoxia-related genes and a concomitant restoration of bile acid metabolism, glycolysis and cholesterol homeostasis in PDX mice treated with the CLDN1 mAb (Fig. 5A). Metabolic reprogramming is a hallmark of carcinogenesis, contributing to tumor progression and therapeutic resistance. The Warburg effect describes the increased uptake of glucose and conversion to lactate in proliferating tumor cells independent of hypoxic conditions.[12] Therefore, we evaluated the effect of the CLDN1 mAb on cancer cell metabolism by performing 3'-deoxy-3'-[^{18}F]-fluorothymidine ([^{18}F]$^{-}$FLT) and 2-deoxy-2-[^{18}F]-fluoro-D-glucose ([^{18}F]-FDG) PET scans of CLDN1 mAb- or control-treated CDX mice. [^{18}F]$^{-}$FLT PET scans of 5 representative CDX mice per group (Fig. 5D) showed reduced uptake of [^{18}F]$^{-}$FLT in CLDN1 mAb- compared to control-treated animals ($p = 0.008$, Fig. 5E left and middle panel). Moreover, total lesion proliferation was markedly reduced in CLDN1 mAb- compared to control-treated mice ($p = 0.03$, Fig.5E, right panel). Meanwhile [^{18}F]-FDG PET scans (Fig. 5F) revealed strongly reduced total lesion glycolysis in Huh7 CDX mice treated with the CLDN1 mAb ($p = 0.02$, Fig. 5G). In contrast, sorafenib treatment did not show any effect on total lesion glycolysis (Fig. 5G). We confirmed the role of CLDN1 in tumor cell metabolism by investigating the effect of the CLDN1 mAb on the induction of a Warburg-like metabolic shift by HCV infection in Huh7.5.1 cells. The flux of lactate and other metabolites was restored to the level of control cells upon CLDN1 mAb treatment (Fig. 5H and Fig. S9A-B). Taken together, these data suggest that CLDN1 drives metabolic tumor reprogramming in different models, including HCC tumors *in vivo*.

CLDN1 mAb alters the tumor cell plasticity by interfering with Notch signaling

The association of CLDN1 overexpression with the progenitor-like stem cell signature suggests a functional role of CLDN1 in tumor cell plasticity. Indeed, gene sets related to liver cancer stemness and EMT were suppressed in CLDN1 mAb-treated PDX mice (FDR <0.05 and FDR <0.001, respectively, Fig. 6A). Supporting this concept, CDX mice treated with the CLDN1 mAb showed a significantly suppressed expression of the stemness and EMT markers EPCAM and fibronectin 1 (Fig. 6B). Linking the molecular effects on EMT with the observed inhibition of cell invasion (Fig. S6C), the CLDN1 mAb strongly suppressed expression of matrix metalloproteinase 14 in cell-based models (p <0.001, Fig. 6C) and CDX mice ($p = 0.01$, Fig. 6D, Fig. S10). To validate the role of CLDN1 in cell plasticity we next assessed the effect of CLDN1 mAb treatment on EMT in patient-derived liver scaffold culture systems, which enable the assessment of cancer therapeutics in a 3D growth microenvironment.[13] To study the effect of CLDN1 mAb on EMT[18] repopulated liver scaffolds were treated with TGFβ (study protocol illustrated in Fig. 6E). The CLDN1 mAb markedly suppressed EMT marker gene expression, including expression of vimentin, fibronectin 1 and snail family transcriptional repressor 2 ($p = 0.005$, $p = 0.008$ and $p = 0.005$, respectively, Fig. 6F). Similar results were obtained in a complementary 3D model system, consisting of Huh7 cells co-cultured with primary cancer-associated fibroblasts in patient liver-derived fibrotic extracellular matrix hydrogel (Fig. S11).

To unravel the molecular drivers of EMT and cell plasticity, we studied the effect of the CLDN1 mAb on Notch signaling – a key regulator of cell differentiation and stemness. Using cell membrane co-immunoprecipitation studies in Huh7 cells, we observed a direct interaction of CLDN1 with JAG1, the upstream inducer of canonical Notch signaling (Fig. 6G, Fig. S13A). The functional relevance of this interaction was confirmed by robust inhibition of Notch cleavage by CLDN1 mAb in HCC cell-based and CDX animal models ($p = 0.03$, Fig. 6H and $p = 0.02$, Fig. 6I, Fig. S12).

Treatment with CLDN1 mAb reprograms TIME in patient-derived HCC spheroids

The TIME has been shown to play an important role in HCC progression and therapeutic resistance.[1] Given the association of CLDN1 expression with an "immune-low" TIME (Fig. 1) and that a well-described signature of immune infiltration predicted response to the CLDN1 mAb[14] (Fig. 4), we next evaluated the effects of the CLDN1 mAb on the TIME of patient-derived HCC tumor spheroids. HCC spheroids (#462, Table S1) were treated with either CLDN1 mAb or an isotype control mAb for 24 h and then subjected to scRNA-seq (Fig. 7A). Unbiased sorting of viable cells enabled sequencing of the transcriptome of all major immune cell types including T cells, macrophages, monocytes and dendritic cells (Fig. 7B, Fig. S13A-G and Table S5). As expected with the short treatment duration, we did not observe any significant difference in the number of any

model) compared to corresponding vehicle control-treated mice (n = 2 mice per model) is shown. (G) Tumor growth for #LI6716 (n = 3 CLDN1 mAb, n = 2 control, $p = 0.004$, Wilcoxon matched pairs test). (H) Tumor growth for #LI6280 (total 24 mice, n = 8 per group treated with 10 mg/ml QIW CLDN1 mAb, 25 mg/ml BIW CLDN1 mAb or control, $p = 0.008$ and $p = 0.004$, Wilcoxon matched-pairs test). (I) Response prediction to CLDN1 mAb treatment in HCC spheroid and PDX models. Bars show NES of significantly (FDR <0.05, Kolmogorov Smirnov test) enriched gene sets. (J) Response prediction to CLDN1 mAb in HCC spheroids by transcriptomic signatures of fibroblasts/angiogenesis as well as an immune infiltrate (FDRs = 0.03 and 0.01, respectively, Kolmogorov-Smirnov test). *p <0.05, **p <0.01, ***p <0.001, ****p <0.0001. CDX, cell line-derived xenograft; FDR, false discovery rate; HCC, hepatocellular carcinoma; mAb, monoclonal antibody; NES, normalized enrichment score; PDX, patient-derived xenograft.

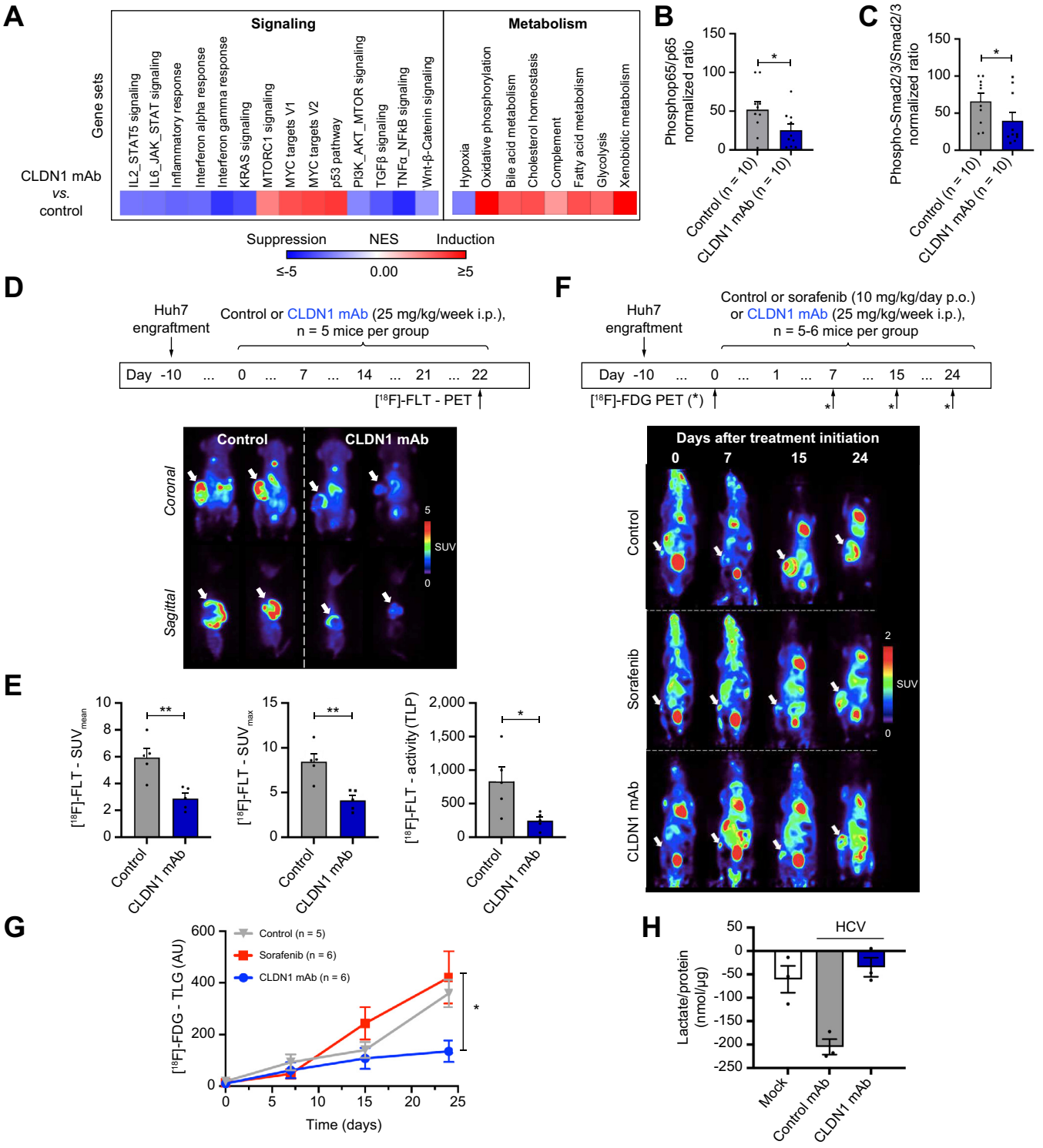

Fig. 5. Impact of CLDN1-specific mAb treatment on tumor signaling and metabolism. (A) Unbiased GSEA analysis of HALLMARK gene sets in tumor tissue of CLDN1 mAb- compared to vehicle control-treated PDX mice (LI6716). Heatmaps show NES of significantly (FDR <0.05, Kolmogorov Smirnov test) altered gene sets. (B, C). Normalized ratio of phospho-p65/p65 and phospho-Smad2/3/Smad 2/3 in CDX mice (n = 5 with two independent protein lysates for each mouse, p <0.05, Mann-Whitney U test). (D) [^{18}F]-FLT PET scan study protocol and representative images showing [^{18}F]-FLT uptake in CLDN1 mAb- or control-treated CDX mice. (E) Quantitative assessment of SUV_{mean} (left panel), SUV_{max} (middle panel), and TLP (activity, right panel) in [^{18}F]-FLT PET scans (n = 5 mice per group, p = 0.008 and p = 0.03, Mann-Whitney U test). (F) [^{18}F]-FDG PET scan study protocol and representative images showing [^{18}F]-FDG uptake in CLDN1 mAb, sorafenib- or control-treated CDX mice. (G) Quantitative assessment of TLG in [^{18}F]-FDG PET scans (n = 5-6 mice per group, *p <0.05, Mann-Whitney U test). (H) Metabolites from CLDN1 or control mAb-treated and HCV-infected or non-infected (Mock) Huh7.5.1^{diff} cells analyzed by mass spectrometry showing liver cell lactate flux. Negative values indicate accumulation outside the cells (one representative experiment, performed in triplicate, **p <0.01, Student's t test). *p <0.05, **p <0.01, ***p <0.001, ****p <0.0001. [^{18}F]-FLT, 3'-deoxy-3'-[^{18}F]-fluorothymidine; [^{18}F]-FDG, 2-deoxy-2-[^{18}F]- fluoro- D-glucose; CDX, cell line-derived xenograft; FDR, false discovery rate; GSEA, gene set-enrichment analysis; HCC, hepatocellular carcinoma; mAb, monoclonal antibody; NES, normalized enrichment score; SUV, standardized uptake value; TLG, total lesion glycolysis; TLP, total lesion proliferation.

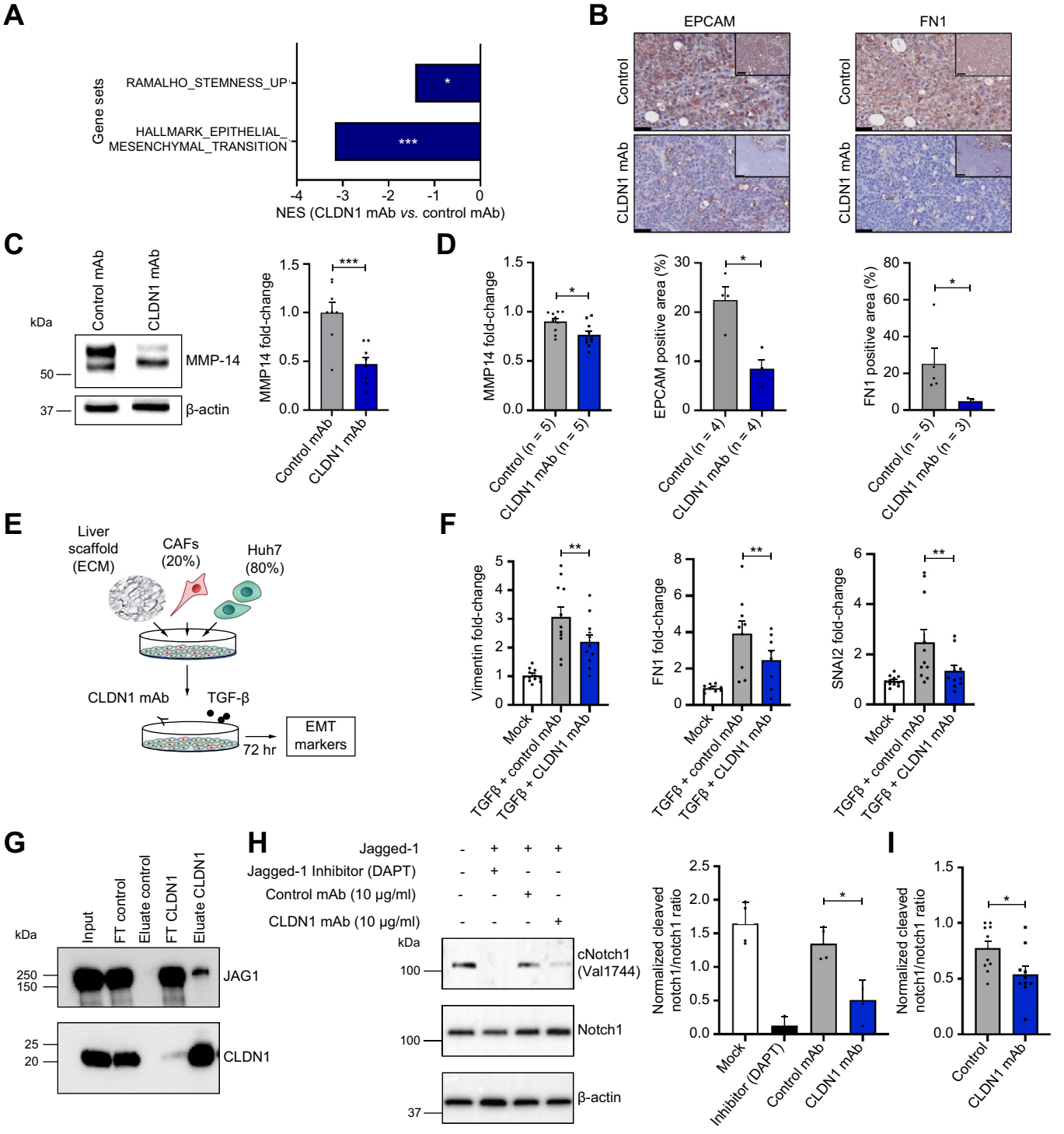

Fig. 6. CLDN1 mAb modulates cancer cell plasticity and fate by interacting with Notch signaling. (A) Significant suppression of gene sets related to EMT and stemness in PDX mice treated with CLDN1 mAb (LI6716: FDR <0.05 and FDR <0.001, Kolmogorov-Smirnov-test). (B) Immunohistochemistry and quantitation of EPCAM and FN1 expression in CDX tumors (n = 5, $p = 0.03$ and $p = 0.04$, Mann-Whitney *U* test, respectively). Scale bars - 1 mm and 200 µm. (C) Inhibition of MMP14 expression in Huh7 spheroids. Left panel: representative immunoblots of MMP14 and β-Actin. Right panel: quantification of normalized MMP14 expression (n = 3 independent experiments in triplicate, $p = 0.001$, Student's *t* test). (D) Quantification of normalized MMP14 expression in CDX HCCs (n = 5, two independent protein lysates for immunoblots, $p = 0.01$, Mann-Whitney *U* test). (E) Patient-derived liver scaffold study protocol. (F) Normalized gene expression of EMT markers vimentin, *FN1* and *SNAI2* in CLDN1 or control mAb-treated Huh7+CAF liver scaffolds (3-4 independent experiments in at least triplicates, $p = 0.005$, $p = 0.008$ and $p = 0.005$, respectively, Wilcoxon signed-rank test). (G) Co-immunoprecipitation of Notch ligand JAG1 and CLDN1 in the cell membrane of Huh7 cells. The western blot shows JAG1 presence in CLDN1 eluate. (H) Inhibition of Notch signaling in Huh7 cells. Left panel: Representative immunoblots of cleaved Notch1 (Val1744), Notch1 and β-actin in Huh7 stimulated with JAG1. Right panel: Normalized ratio of cleaved Notch1/Notch1 protein expression (n = 3, $p = 0.03$, Mann-Whitney *U* test). (I) Normalized ratio of cleaved Notch1/Notch1 in HCCs from CDX mice (5 mice per group and two independent lysates each), $p = 0.02$, Mann-Whitney *U* test). Bars show mean ±SEM. *p <0.05, **p <0.01, ***p <0.001, ****p <0.0001. CAF, cancer-associated fibroblast; CDX, cell line-derived xenograft; EMT, epithelial-mesenchymal transition; FDR, false discovery rate; HCC, hepatocellular carcinoma; mAb, monoclonal antibody.

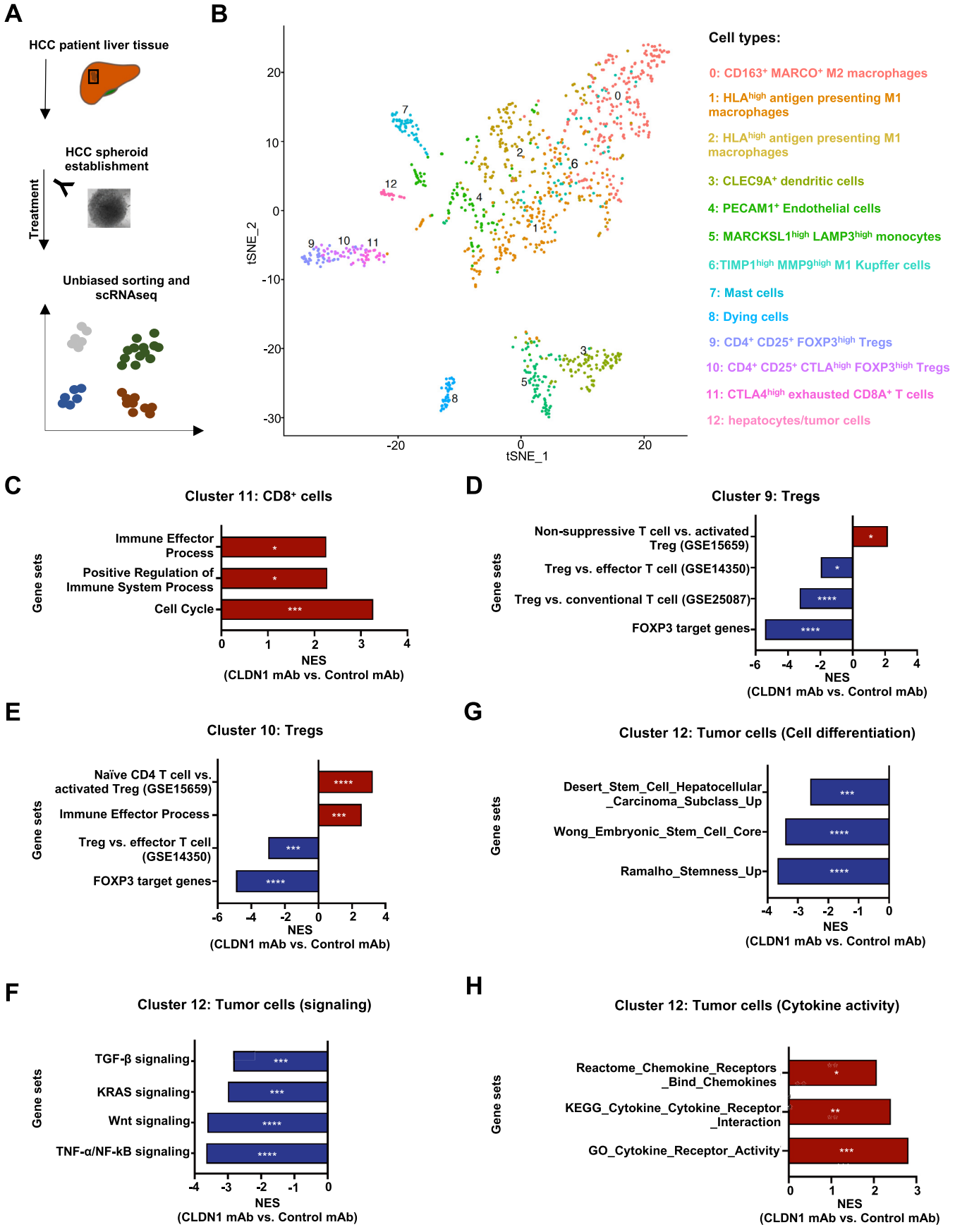
A
HCC patient liver tissue
HCC spheroid establishment
Treatment
Unbiased sorting and scRNAseq
B
tSNE_2
tSNE_1
Cell types:
0: CD163+ MARCO+ M2 macrophages
1: HLAhigh antigen presenting M1 macrophages
2: HLAhigh antigen presenting M1 macrophages
3: CLEC9A+ dendritic cells
4: PECAM1+ Endothelial cells
5: MARCKSL1high LAMP3high monocytes
6:TIMP1high MMP9high M1 Kupffer cells
7: Mast cells
8: Dying cells
9: CD4+ CD25+ FOXP3high Tregs
10: CD4+ CD25+ CTLAhigh FOXP3high Tregs
11: CTLA4high exhausted CD8A+ T cells
12: hepatocytes/tumor cells
C
Cluster 11: CD8+ cells
Gene sets
Immune Effector Process
Positive Regulation of Immune System Process
Cell Cycle
NES
(CLDN1 mAb vs. Control mAb)
D
Cluster 9: Tregs
Non-suppressive T cell vs. activated Treg (GSE15659)
Treg vs. effector T cell (GSE14350)
Treg vs. conventional T cell (GSE25087)
FOXP3 target genes
E
Cluster 10: Tregs
Naïve CD4 T cell vs. activated Treg (GSE15659)
Immune Effector Process
Treg vs. effector T cell (GSE14350)
FOXP3 target genes
G
Cluster 12: Tumor cells (Cell differentiation)
Desert_Stem_Cell_Hepatocellular_Carcinoma_Subclass_Up
Wong_Embryonic_Stem_Cell_Core
Ramalho_Stemness_Up
F
Cluster 12: Tumor cells (signaling)
TGF-β signaling
KRAS signaling
Wnt signaling
TNF-α/NF-kB signaling
H
Cluster 12: Tumor cells (Cytokine activity)
Reactome_Chemokine_Receptors_Bind_Chemokines
KEGG_Cytokine_Cytokine_Receptor_Interaction
GO_Cytokine_Receptor_Activity

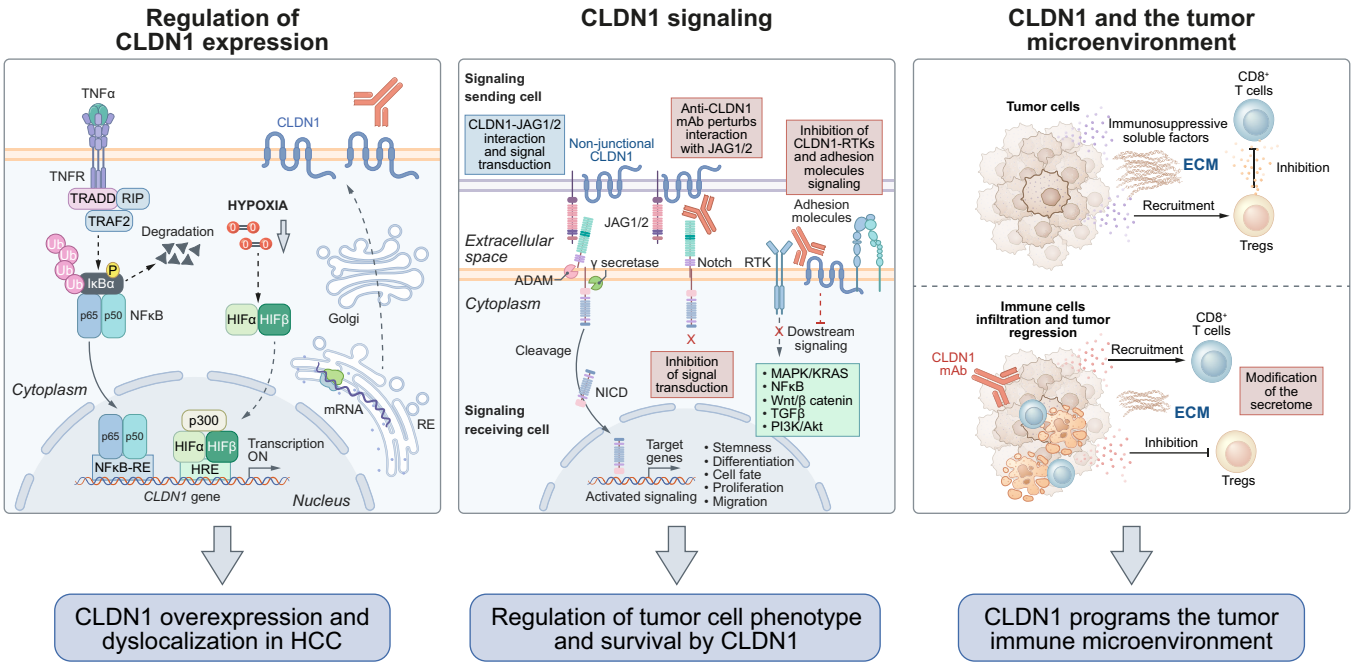

Fig. 8. Mechanistic model for CLDN1-targeting therapies. Left: Upregulation of CLDN1 expression by TNFα–NF–κB signaling and hypoxia/HIF1α (Fig. 1, 2). Anti-CLDN1 antibodies bind to non-junctional CLDN1 on the tumor cell surface. Middle: Anti-CLDN1 treatment interferes with tumor cell signaling regulating tumor stemness, differentiation, cell fate, proliferation and migration (Fig. 4-6) by perturbating the JAG-Notch pathway (Fig. 6). Other downstream targets may be mediated via non-canonical Notch signaling or by CLDN1 interaction/cross-talk with other adhesion molecules or RTKs.[5,19] Right: High CLDN1 expression is associated with an immune-low or inactive TIME (Fig. 1, 7). The change of the tumor cell phenotype by mAb treatment leads to activation of T cells in the TIME likely by altering the tumor cell secretome and/or metalloproteinases (Fig. 6). Ab-mediated inhibition of liver fibrosis described previously[20] may further contribute to treatment response. HCC, hepatocellular carcinoma; mAb, monoclonal antibody; RTK, receptor tyrosine kinase; TIME, tumor immune microenvironment.

immune cell subsets (Fig. S13A). However, in CLDN1 mAb-treated patient HCC spheroids, CD8$^+$ T cells showed enrichment of genes associated with immune effector function and proliferation (Fig. 7C). In contrast, in two immunosuppressive regulatory T cell clusters, FOXP3 target genes were strongly downregulated while genes associated with an immune effector function were upregulated (Fig. 7D,E). Since *CLDN1* expression was not detectable in T cells (Fig. S13D,F) these effects are most likely due to a direct impact of exposed CLDN1 on tumor cells.

GSEA on HCC sorted tumor cells confirmed the downregulation of TGFβ-, KRAS, Wnt- and TNFα-signaling pathways whose activation has been associated with an immune TIME[15] (Fig. 7F). Furthermore, gene sets associated with immunogenic cytokine activity were suppressed in tumor cells (Fig. 7H).

Altogether, these data suggest that exposed CLDN1 expressed on tumor cells may dictate an immunosuppressive TIME in HCC that can be reverted by the CLDN1 mAb into an immunostimulatory TIME. These data thus provide a rationale for combining CLDN1 mAbs with immune checkpoint inhibitors in HCC.

Discussion

Applying patient-derived *ex vivo* and *in vivo* models and a highly specific mAb, we identified CLDN1 as a novel therapeutic target for HCC. CLDN1 mAb treatment inhibits tumor growth and its phenotype (Fig. 8) by (a) targeting CLDN1 upregulated by TNFα and hypoxia (Fig. 1,2); (b) suppressing cancer cell stemness and EMT, a hallmark of HCC tumors with high invasive capacity, therapeutic resistance and poor prognosis (Fig. 4); (c) reprogramming tumor metabolism, a feature of cancer cells that determines cell survival, hyperplastic growth and evasion from immune responses (Fig. 5); (d) inducing apoptosis (Fig. 4, 6); and (e) altering the TIME with enhancement of antitumor activity (Fig. 7).

Fig. 7. scRNAseq of patient-derived HCC spheroids suggests that CLDN1 mAb treatment modulates T cell effector activity. (A) Study protocol of scRNA-seq on sorted immune cells derived from CLDN1 or control mAb-treated HCC spheroids (n = 10-20 spheroids per group). (B) 2D-visualization of single-cell transcriptomics of cells sorted from CLDN1 *vs.* control mAb-treated HCC spheroids using t-SNE maps. (C) Significant upregulation of gene sets related to immune effector processes and proliferation in CD8$^+$ T cells derived from CLDN1 *vs.* control mAb-treated HCC spheroids. (D) Significant suppression of gene sets specific for Tregs and upregulation of markers of non-suppressive T cells in CD4$^+$ CD25$^+$ FOXP3^{high} Tregs. (E) Significant suppression of gene sets specific for Tregs and upregulation of genes related to immune effector processes as well as naïve CD4$^+$ T cells in CD4$^+$ CD25$^+$ CTLA4^{high} FOXP3^{high} Tregs. (F) Significantly suppressed signaling gene sets in tumor cells derived from CLDN1 *vs.* control mAb-treated HCC spheroids. (G) Suppression of gene sets related to stemness in tumor cells derived from CLDN1- *vs.* control mAb-treated HCC spheroids. (H) Enrichment of gene sets related to cytokine production in tumor cells derived from CLDN1 *vs.* control mAb-treated spheroids. Horizontal bars indicate NES; *FDR <0.05, **<0.01, ***<0.001, ****< 0.0001. FDR, false discovery rate; HCC, hepatocellular carcinoma; mAb, monoclonal antibody; scRNA-Seq, single-cell RNA-sequencing; Tregs, regulatory T cells; t-SNE, t-distributed stochastic neighbor embedding.

Mechanistic studies indicated that inhibition of Notch signaling via direct interactions between CLDN1 and JAG1 likely plays a role in the observed effects on tumor cell fate (Fig. 6). Since we did not observe a significant induction of Notch effector genes in the PDX HCC transcriptome LI6716 (Fig. 5A), it is conceivable that Notch signaling is either an early event in the signal cascade or that perturbation of Notch signaling is heterogenous in individual tumors. The Notch pathway has been identified as a key regulator of cell differentiation, fate and survival and several functional and clinical studies have shown that the Notch pathway plays a role in the pathogenesis of HCC.[16,17] Since Notch signaling has also been identified as a regulator of innate and adaptive immune responses,[18] its perturbation by CLDN1 mAb treatment may also contribute to the observed effects on the TIME (Fig. 7).

The observed effects on NF-kB, Wnt-β-catenin and P3IK signaling (Fig. 6A) may be mediated via non-canonical Notch signaling or by signal transduction of other cell membrane molecules shown to interact/cross-talk with CLDN1.[5,19,20] The CLDN1 mAb-induced alteration of tumor cell plasticity and its related immunomodulatory effects highlight potential opportunities for combining CLDN1 mAb treatment with immune-oncological approaches and multi-kinase inhibitors.[1]

HCC arises almost exclusively in the context of liver fibrosis and chronic inflammation.[21] The stage of liver fibrosis hereby represents a key factor for patient outcome.[1] In addition to the tumor suppressive effects of the CLDN1 mAb demonstrated in this study, we previously showed that CLDN1-targeting mAbs suppress liver fibrosis.[20] While HCC treatment strategies are frequently limited by the degree of cirrhosis,[1] the combined anti-fibrotic and tumor suppressive effects of CLDN1 mAbs provide a unique opportunity to target not only tumor growth but also fibrosis and *de novo* HCC development in the non-tumorous fibrotic microenvironment.[1]

Furthermore, this study provides prediction markers to guide patient selection. Upregulation of EMT as well as signaling pathways implicated in stemness such as Wnt/β-catenin and Hedgehog signaling[22] predicted response of HCC tumors to the experimental CLDN1 mAb treatment.

Our data obtained here and in previous studies demonstrate that the administration of the antibody is safe without detectable adverse and off-target effects.[5,23] The absence of toxicity and off-target effects are likely due to the specific binding of the mAb to NJ-CLDN1 and not to TJ-CLDN1.[5,20]

Collectively, our data provide robust pre-clinical proof-of-concept for CLDN1 mAbs as potential first in-class compounds that could break the plateau of limited treatment response in advanced HCC, improving the outlook for patients who currently have a poor prognosis.

Affiliations

[1]Université de Strasbourg, Strasbourg, France; [2]Inserm, U1110, Institut de Recherche sur les Maladies Virales et Hépatiques, Strasbourg, France; [3]CNRS, Institut Pluridisciplinaire Hubert Curien UMR 7178, Strasbourg, France; [4]Institut Hospitalo-Universitaire, Pôle Hépato-digestif, Nouvel Hôpital Civil, Strasbourg, France; [5]Division of Chronic Inflammation and Cancer, German Cancer Research Center, Heidelberg, Germany; [6]Alentis Therapeutics, Basel, Switzerland; [7]Department of Functional Genomics and Cancer, Institut de Génétique et de Biologie Moléculaire et Cellulaire, CNRS/INSERM/UDS, Illkirch, France; [8]Department of Pathology, University Hospital of Geneva, Switzerland. [9]Massachusetts General Hospital Cancer Center, Harvard Medical School, Charlestown, MA, USA; [10]Liver Tumor Translational Research Program, Harold C. Simmons Comprehensive Cancer Center, Division of Digestive and Liver Diseases, University of Texas Southwestern Medical Center, Dallas, TX, USA; [11]Cancer Research Center of Lyon (CRCL), UMR Inserm 1052 CNRS 5286 Mixte CLB, Université de Lyon 1 (UCBL1), Lyon, France; [12]Institut Universitaire de France (IUF), Paris, France

Abbreviations

[^{18}F]-FDG, 2-deoxy-2-[^{18}F]-fluoro-D-glucose; [^{18}F]$^{-}$FLT= 3'-deoxy-3'-[^{18}F]-fluorothymidine; CDX, cell line-derived xenograft; ECM, extracellular matrix; EMT, epithelial-mesenchymal transition; FDR, false-discovery rate; GSEA, gene set enrichment analysis; HCC, hepatocellular carcinoma; mAb, monoclonal antibody; NJ-CLDN1, non-junctional CLDN1; PDX, patient-derived xenograft; RNA-seq, RNA-sequencing; scRNAseq, single-cell RNA sequencing; TJs, tight junctions; TIME, tumor immune microenvironment; TME, tumor microenvironment.

Financial support

The authors acknowledge the following financial support: European Research Council Grant ERC-AdG-2014 *HEPCIR* (T.F.B. and Y.H.); European Research Council Grant ERC-AdG-2020 *FIBCAN* (T.F.B. and Y.H.); European Research Council Grant ERC-PoC-2016 *PRELICAN* (T.F.B.); European Research Council Grant ERC-PoC-2018 *HEPCAN* (T.F.B.); European Research Council Consolidator grant *HepatoMetabopath* (M.H.); ARC Grant *TheraHCC2.0* IHUARC IHU201301187 (T.F.B.); ANRS Grant ECTZ103701 (T.F.B.); SATT Conectus, University of Strasbourg (CANCLAU) (T.F.B.); French National Research Agency DELIVER (ANR-21-RHUS-0001) within the France 2030 program and LABEX ANR-10-LABX-0028_*HEPSYS* (T.F.B.); Grand-Est Region (M.M. and N.A.); German Research Foundation (DFG) RO 5983/1-1 (N.R.). This work of the Interdisciplinary Thematic Institute IMCBio, as part of the ITI 2021-2028 program of the University of Strasbourg, CNRS and Inserm, was further supported by IdEx Unistra (ANR-10-IDEX-0002), and by SFRI-STRAT'US project (ANR 20-SFRI-0012) and EUR IMCBio (ANR-17-EURE-0023) under the framework of the French Investments for the Future Program and the France 2030 program.

Conflict of interest

Inserm, the University of Strasbourg and the Institut Hospitalo-Universitaire have filed patent applications for the use of anti-claudin-1 monoclonal antibodies for the treatment of liver disease, NASH and HCC (PCT/EP2016/055942, PCT/EP2017/056703) which have been licensed to Alentis Therapeutics Basel. T.F.B. is a founder, shareholder and advisor for Alentis. A.T., R.I., G.E., H.E.S. GT and M.M. are employees of Alentis Therapeutics. Y. H., T. S. and C. S. are shareholders of Alentis Therapeutics.

Please refer to the accompanying ICMJE disclosure forms for further details.

Authors' contributions

T.F.B. initiated and led the study. N.R., S.C, F.H.D, E.C., C.S., L.M., J.L., B.N., M.B.Z., S. M., P.L. and T.F.B. designed experiments and analyzed data. N.R., S.C., C.T., F.H.T.D., F.D.Z., S.C.D., S.B., C.P., M.F., T.R., Z.N., A.L., M.A.O. and N.A. performed experiments and analyzed data. G. E. engineered humanized mAbs. M.M., R.M., L.M., M.F.V and N.Br. performed and analyzed animal experiments. M.M. and P.M. performed and analyzed PET-Scan experiments. R.I., T.S., G.E. and M.M. designed PDX mouse model studies. H.E.S. performed gene expression analyses. A.S., S.M. and G.T. designed or performed immunohistochemistry analyses. F.J. performed computational analyses. M.H., I.D., A.T., Y.H. and N.Ba. gave critical conceptual input. E.F. and P.P. recruited and prepared patient liver tissues for *ex vivo* experiments. N.R., E.C., S.C., M.M. and N.A. designed figures and tables. N.R., J.L. and T.F.B. wrote the manuscript. All authors read and approved the final manuscript to be submitted.

Data availability statement

Transcriptomic data acquired and reported in this paper has been deposited on GEO (GSE196393). All other data associated with this paper are available upon request to the corresponding author.

Acknowledgments

The authors thank the CRB (Centre de Ressources Biologiques-Biological Resource Centre) of the Strasbourg University Hospitals for the management of

patient-derived liver tissue. The authors thank Dr. D. Root (Broad Institute of MIT and Harvard, Cambridge, MA) for providing expression plasmids for lentiviruses and sgRNAs for CLDN1 KO and Prof. Gerhard Cristofori (University of Basel) for the gift of Huh7 cells, Drs. F. Chisari (Scripps) and C. Rice (Rockefeller University) for providing Huh7.5.1 cells and Dr. R. Bartenschlager (University of Heidelberg) for providing HCV Jc1 strain, Thomas Cagarelli and Dr. Aurélie Bornand (University Hospital Geneve) for histopathological analyses and Dr. Olga Koutsopoulos (Inserm U1110, U Strasbourg) for helpful discussions, project management and support in fundraising. The authors thank the entire personnel of the CYRCe platform (IPHC, France) for their contribution to the PET experiments.

Supplementary data

Supplementary data to this article can be found online at https://doi.org/10.1016/j.jhep.2022.10.011.

References

Author names in bold designate shared co-first authorships

[1] Llovet JM, Kelley RK, Villanueva A, Singal AG, Pikarsky E, Roayaie S, et al. Hepatocellular carcinoma. Nat Rev Dis Primers 2021;7:6.
[2] Finn RS, Qin S, Ikeda M, Galle PR, Ducreux M, Kim T-Y, et al. Atezolizumab plus Bevacizumab in unresectable hepatocellular carcinoma. N Engl J Med 2020;382:1894–1905.
[3] Calderaro J, Ziol M, Paradis V, Zucman-Rossi J. Molecular and histological correlations in liver cancer. J Hepatol 2019;71:616–630.
[4] **Qin S**, **Jiang J**, Lu Y, Nice EC, Huang C, Zhang J, et al. Emerging role of tumor cell plasticity in modifying therapeutic response. Signal Transduct Target Ther 2020;5:228.
[5] Mailly L, Xiao F, Lupberger J, Wilson GK, Aubert P, Duong FHT, et al. Clearance of persistent hepatitis C virus infection in humanized mice using a claudin-1-targeting monoclonal antibody. Nat Biotechnol 2015;33:549–554.
[6] Uhlén M, Fagerberg L, Hallström BM, Lindskog C, Oksvold P, Mardinoglu A, et al. Proteomics. Tissue-based map of the human proteome. Science 2015;347:1260419.
[7] **Boyault S**, **Rickman DS**, **de Reyniès A**, Balabaud C, Rebouissou S, Jeannot E, et al. Transcriptome classification of HCC is related to gene alterations and to new therapeutic targets. Hepatology 2007;45:42–52.
[8] Pinyol R, Montal R, Bassaganyas L, Sia D, Takayama T, Chau G-Y, et al. Molecular predictors of prevention of recurrence in HCC with sorafenib as adjuvant treatment and prognostic factors in the phase 3 STORM trial. Gut 2019;68:1065–1075.
[9] Song Y, Kim J-S, Kim S-H, Park YK, Yu E, Kim K-H, et al. Patient-derived multicellular tumor spheroids towards optimized treatment for patients with hepatocellular carcinoma. J Exp Clin Cancer Res 2018;37:109.
[10] **Xu C**, **Li X**, Liu P, Li M, Luo F. Patient-derived xenograft mouse models: a high fidelity tool for individualized medicine. Oncol Lett 2019;17:3–10.
[11] Roehlen N, Roca Suarez AA, el Saghire H, Saviano A, Schuster C, Lupberger J, et al. Tight junction proteins and the biology of hepatobiliary disease. Int J Mol Sci 2020:21.
[12] vander Heiden MG, Cantley LC, Thompson CB. Understanding the Warburg effect: the metabolic requirements of cell proliferation. Science 2009;324:1029–1033.
[13] Miyauchi Y, Yasuchika K, Fukumitsu K, Ishii T, Ogiso S, Minami T, et al. A novel three-dimensional culture system maintaining the physiological extracellular matrix of fibrotic model livers accelerates progression of hepatocellular carcinoma cells. Sci Rep 2017;7:9827.
[14] Bagaev A, Kotlov N, Nomie K, Svekolkin V, Gafurov A, Isaeva O, et al. Conserved pan-cancer microenvironment subtypes predict response to immunotherapy. Cancer Cell 2021;39:845–865.e7.
[15] Llovet JM, Castet F, Heikenwalder M, Maini MK, Mazzaferro V, Pinato DJ, et al. Immunotherapies for hepatocellular carcinoma. Nat Rev Clin Oncol 2022;19:151–172.
[16] Zhu C, Ho Y-J, Salomao MA, Dapito DH, Bartolome A, Schwabe RF, et al. Notch activity characterizes a common hepatocellular carcinoma subtype with unique molecular and clinicopathologic features. J Hepatol 2021;74:613–626.
[17] Villanueva A, Alsinet C, Yanger K, Hoshida Y, Zong Y, Toffanin S, et al. Notch signaling is activated in human hepatocellular carcinoma and induces tumor formation in mice. Gastroenterology 2012;143:1660–1669.e7.
[18] Radtke F, MacDonald HR, Tacchini-Cottier F. Regulation of innate and adaptive immunity by Notch. Nat Rev Immunol 2013;13:427–437.
[19] **Zona L**, **Lupberger J**, Sidahmed-Adrar N, Thumann C, Harris HJ, Barnes A, et al. HRas signal transduction promotes hepatitis C virus cell entry by triggering assembly of the host tetraspanin receptor complex. Cell Host Microbe 2013;13:302–313.
[20] **El Saghire H**, **Saviano A**, **Roehlen N**, Crouchet E, Duong FHT, Jühling F et al. Abstract of The International Liver Congress TM 2021 June 23-26, 2021. Abstract GS-2069.
[21] Baglieri J, Brenner DA, Kisseleva T. The role of fibrosis and liver-associated fibroblasts in the pathogenesis of hepatocellular carcinoma. Int J Mol Sci 2019;20.
[22] Liu Y-C, Yeh C-T, Lin K-H. Cancer stem cell functions in hepatocellular carcinoma and comprehensive therapeutic strategies. Cells 2020;9.
[23] Colpitts CC, Tawar RG, Mailly L, Thumann C, Heydmann L, Durand SC, et al. Humanisation of a claudin-1-specific monoclonal antibody for clinical prevention and cure of HCV infection without escape. Gut 2018;67:736–745.